Electrical properties of biomorphic SiC ceramics and SiC/Si composites fabricated from medium density fiberboard

T.S. Orlova (a), V.V. Popov (a), J. Quispe Cancapa (b), D. Hernández Maldonado (b), E. Enrique Magarino (b), F.M. Varela Feria (b), A. Ramírez de Arellano (b), J. MartínezFernández (b)

(a)IoffePhysicotechnical Institute, Russian Academy of Sciences, Politekhnicheskayaul. 26, St. Petersburg, 194021 Russia

(b) Dpto. Física de la Materia Condensada-ICMSE, Universidad de Sevilla-CSIC, Sevilla 41080 Spain

Abstract

A study has been made of the dependences of the electrical resistivity and the Hall coefficient on the temperature in the range 1.8–1300 K and on magnetic fields of up to 28 kOe for the biomorphic SiC/Si (MDF-SiC/Si) composite and biomorphic porous SiC (MDF-SiC) based upon artificial cellulosic precursor (MDF – medium density fiberboards). It has been shown that electric transport in MDF-SiC is effected by carriers of n-type with a high concentration of ∼1020 cm−3 and a low mobility of ∼0.4 cm2 V−1 s−1. The specific features in the conductivity of MDF-SiC are explained by quantum effects arising in disordered systems and requiring quantum corrections to conductivity. The TEM studies confirmed the presence of disordering structural features (nanocrystalline regions) in MDF-SiC. The conductivity of MDF-SiC/Si composite originates primarily from Si component in the temperature range 1.8–500 K and since ∼500 to 600 K the contribution of MDF-SiC matrix becomes dominant.

Keywords

C. Electrical properties; BiomorphicSiC;SiC/Si composite; Electron microscopy

1. Introduction

The studies of electrical properties of silicon carbide (SiC) ceramics and SiC-based composites have tremendous scientific significance and practical interest as well. Due to their high performance characteristics at high temperatures and good resistance to corrosive environments the SiC materials are promising to be used for heater elements, resistance thermometers and thermoelectric power generators in space, automotive and energy transformation industries.1

The main fabrication processes of SiC ceramics are carbothermic reduction of SiO2,2 reactive compaction,3 and 4 and hot sintering.5 and 6 Recently, natural wood-derived biomorphic SiC (bio-SiC) ceramics have been a matter of interest.7, 8, 9, 10, 11, 12, 13 and 14 The processing technique of porous SiC ceramics from wood involves the pyrolysis of natural wood precursors,

followed by the infiltration of molten silicon to form silicon carbide (SiC), retaining the initial wood porous structure.9, 10, 11, 12, 13 and 14 Some residual Si remains in cellular pores forming thereby SiC/Si composite. The pure porous material, bio-SiC, is produced from the SiC/Si composite by etching silicon out of the channel pores.15 Both biomorphic SiC/Si composite and porous SiC ceramic (the composite matrix) have highly anisotropic structure, replicating the cellular structure of natural wood (cellular channel pores elongated along the tree growth direction). Some amount of unreacted carbon is also present in biomorphic SiC/Si composite as well as in porous bio-SiC.13

The bio-SiC has several advantages over conventional SiC. It presents relatively light material with open porous structure, which possesses excellent mechanical properties in compression and flexure.16 The technology of its fabrication allows for relatively easy production of complex shapes by using preliminary machining of biomorphic carbon precursor.12 The processing of bio-SiC is much cheaper because it occurs at temperatures that are much lower than those required for SiC sintering or hot-pressing techniques. The latter requires temperatures exceeding 2000 °C.4 and 5 The structure and resulting properties, mechanical ones at least, of bio-SiC and bio-SiC/Si strongly depend on the original wood precursor used.17

Investigation of the electrical transport properties of this new class of materials – biomorphic natural wood-derived SiC/Si composites and porous bio-SiC has been recently attracting considerable attention. For example, the electric resistivity ρ of biomorphic SiC/Si composites derived from sapele,18 white eucalyptus 19, 20 and 21 and beech22 was measured in the temperature range 5–300 K. In Ref.23, the temperature range of measurement of the dependence ρ(T) was extended to 950 K for the SiC/Si composites fabricated from white eucalyptus. These studies revealed that the electrical resistivity of biomorphic SiC/Si is anisotropic, i.e. there is a difference between the resistivity ρII measured along the axial direction (parallel to the tree growth direction) and the resistivity ρ⊥ measured along the transverse direction. In the temperature range 4.2–300 K, both temperature dependences ρII(T) and ρ⊥(T) follow semimetallic pattern: the electrical resistivity varies insignificantly at low temperatures and increases starting from ∼100 K. ρII of the biomorphic SiC/Si composites at room temperature varies in the range 10−3 to 10−2 Ω cm. The conductivity of biomorphic SiC/Si composites (derived from eucalyptus21 and beech22) was found to originate primarily from Si component and to be provided by carries of p-type with concentration of the order of 1019 cm−3 and high mobility (∼103 cm2 V−1 s−1 at 4.2 K).22 All kinds of wood taken as initial precursors in the above considered works belong to the wood with open porosity.24

However, ρ(T) dependences measured for bamboo wood-derived SiC/Si composite exhibited a semiconducting pattern over a wide temperature range (25–1000 K)25 that is contrary to metallic ρ(T) behaviour of biomorphic SiC/Si from sapele,18 eucalyptus 19, 20 and 21 or beech.22 This difference seems to be explained by the specificity of bamboo structure. As it was noted in Ref.24 carbon preforms from bamboo contain a combination of channel pores and closed cells that impede the complete infiltration of Si. As a result interconnecting Si-filled channels network probably is not formed. This can also lead to a large amount of unreacted carbon which can form own conducting percolation paths.

The resistivity of porous bio-SiC (from eucalyptus21 and beech22) at low temperatures (4.2–300 K) is several orders of magnitude higher than the resistivity of the respective SiC/Si composites. The ρ(T) dependences of the bio-SiC demonstrate semiconducting behaviour in the range 4.2–300 K. The electrical transport in beech-derived bio-SiC is effected by n-type carriers with a high concentration of ∼1019 cm−3 and a low mobility of ∼1 cm2 V−1 s−1.22 It has been concluded22 that the electrical transport in the natural beech-derived SiC occurs similarly to the transport in strongly disordered semiconductors and could be described with theory of quantum corrections to the conductivity.26

Nowadays precursors which could be alternative to the natural wood are considered to be promising for processing bio-SiC and bio-SiC/Si materials. These are artificial compacted fiberboards or, more specifically, medium density fiberboards (MDF). Processing technology of MDF-based biomorphic SiC (MDF-SiC) and respective SiC/Si (MDF-SiC/Si) composite is similar to that used for natural wood precursors.27 and 28 The MDF-SiC and MDF-SiC/Si have some advantages compared with similar materials processed from natural wood precursor. Upon carbonization, the homogeneity and consistency of fiber-boards result in the formation of a consistent, low-coast hard carbon.29 Because of better homogeneity carbonized fiberboards can be more easily machined into complicated shapes compared with carbonized woods.29 Since MDF boards are formed under controlled conditions, MDF-SiC can possess reproducible homogenous structure unlike natural wood-derived SiC materials the structure of which depends on yearly rings, climate factors, etc. Processing of MDF by pressing allows a choice of density and porosity of the precursor that can modify functional characteristics of final MDF-SiC. There are only a few papers devoted to mechanical properties of MDF-SiC and MDF-SiC/Si composites.27 and 28 Physical properties, specifically electrical ones, of MDF-SiC have not been studied, at all.

The aim of the present work is to investigate electrical properties of porous bio-SiC ceramic and bio-SiC/Si composites both obtained from MDF precursors. Measurements have been made of temperature dependences of the electrical resistivity, as well as the Hall coefficient in a temperature range of 1.8–300 K and magnetic fields of up to 28 kOe. The type and concentration of carriers in MDF-SiC were determined from measurements of the Hall coefficient. Electrical properties of MDF-SiC/Si and MDF-SiC are compared with those of similar biomorphic materials fabricated from natural wood (eucalyptus, beech, bamboo).

In addition, we also present some of our preliminary data on resistivity-temperature behaviour of MDF-SiC and MDF-SiC/Si materials at elevated temperatures (from 300 to 1300 K).

2. Experimental procedure

Porous biomorphic SiC ceramic and SiC/Si composite, both derived from MDF boards, have been prepared. A commercial medium density (0.6–0.8 g/cm3) MDF boards were chosen as precursor. The processing technique of MDF-based SiC (hereinafter MDF-SiC) and SiC/Si (MDF-SiC/Si) composites included several stages. The processing technology is presented in details in Refs.27 and 28. Briefly, first a MDF piece of 50 mm × 30 mm × 30 mm was pyrolized at 1050 °C in flowing argon. As a result, the biocarbon preform (MDF-C) was obtained.

Unlike the biocarbon obtained by pyrolysis of the natural wood (eucalyptus, beech, sapele, pine), which has open channel pores along the tree growth direction, the MDF-C has more homogeneous structure.28 An example of the microstructure of the MDF-C is shown in Fig. 1. Samples of MDF-C were cut with dimensions of 3 mm × 3 mm × 20 mm, the long dimension being perpendicular to the direction of the load application in MDF pressing.

Each sample of MDF-C perform was infiltrated with an excess of Si to the stoichiometric amount needed for all the C amount in the perform. The final SiC/Si composites were formed.

Pure biomorphic MDF-SiC samples derived from MDF boards were obtained by etching silicon away with a mixture of hydrofluoric and nitric acids.15

The dependences of electrical resistivity and of the Hall constant R on temperature and magnetic field H were measured by the standard four-probe technique. In these measurements the electric current was passed along the long side of the sample, i.e., perpendicular to the pressing direction in the parent MDF board processing. The concentration and mobility of charge carriers were determined by Hall method.

The microstructure of bio SiC (MDF) sample was characterized by scanning and transmission electron microscopy (SEM and TEM) using a Philips XL30 scanning electron microscope and a Philips CM-200 transmission electron microscope respectively (Electron Microscopy Service, CITIUS, University of Seville, Spain). Samples for SEM and TEM observations were fabricated following conventional techniques.

3. Results and discussion

3.1. Low-temperature studies

Low-temperature (4.2–300 K) studies were made on the samples obtained on the base of the initial MDF board with density 0.8 g/cm3. The excess of Si taken for the filtration was determined by ratio PSi = 3.5 Pc where PSi and Pc are the weight fractions of Si and MDF-C. Such ratio provides approximately 30 vol.% of remaining Si in the resulting SiC/Si composites after the infiltration.

3.1.1. MDF-derived carbon precursor

Since all biomorphic SiC/Si composites as well as pure porous biomorphic SiC materials derived from natural wood or from MDF contain some amount of residual carbon,11 first we studied resistivity-temperature dependences ρ(T) of MDF-C preforms which were used for processing MDF-SiC/Si composites and porous MDF-SiC ceramics. In Fig. 2 the resistivity-temperature ρ(T) dependences of MDF-C preforms are compared with those of biocarbon preforms pyrolized from natural wood (eucalyptus30 and pine31) at the same temperature of carbonization ~1000 °C. Fig. 2a corresponds to the porous biomorphic carbon samples, whereas in Fig. 2b the ρ(T) dependences are recalculated with correction for the porosity. To make correction for the porosity it is necessary to refer the resistance to the working volume (cross-section) participating in charge transfer. In the case of the wood-derived biocarbon samples (eucalyptus30 and pine31) with channel porosity, the resistivity along the tree growth direction with correction for the porosity was found according to the expression.23

$\rho_1=\rho(1-P)$.

Here, ρ and ρ1 are the resistivities without and with the correction for the porosity of the sample, respectively, and P is the porosity. For MDF-C samples, in a rough approximation, we could assume that in the cross-section of the sample also only an area S1 = (1 − P)S transfers the current. Here S and S1 are the cross-sections of the sample without and with correction for the porosity, respectively. The obtained ρ1(T) dependence for MDF-C with allowance for porosity is shown in Fig. 2b (curve 1). All the ρ(T) dependences demonstrate similar character of semiconducting pattern. The values of ρ1 in the temperature range 5–300 K for MDF-C are very close to those for the pine-derived biocarbon. It is known that commercial MDF boards are mainly produced from pine fiber precursors. 32 and 33

3.1.2. MDF-derived SiC/Si composite and porous MDF-SiC

Fig. 3a displays typical temperature dependence of electrical resistivity ρ of MDF-SiC/Si composite. The value of ρ grows with increasing temperature from about 50 to 300 K. Such behaviour is a signature of metallic conduction. However for lower temperatures MDF-SiC/Si composite shows weak semiconducting behaviour. Similar behaviour was also observed for biomorphic SiC/Si composite processed on the base of natural wood of different type. For comparison, ρ(T) dependences of biomorphic SiC/Si composites derived from natural wood (eucalyptus21 and beech22) are presented in Fig. 3b. For SiC/Si composites derived from the same type of wood, the value of resistivity at room temperature, ρ300, varies from 0.002 to 0.02 Ω cm. 18, 19, 20 and 21 It is dependent on the volume fraction of Si and residual porosity in the composite.21 As a whole, the ρ(T) dependences and the resistivity at room temperature for MDF-SiC/Si composites are very similar to those of biomorphic SiC/Si derived from the wood with open porosity, like eucalyptus,21 beech,22 sapele,18 but very different from those of biomorphic SiC/Si derived from Indian bamboo.25 The ρ(T) dependence of bamboo-derived SiC/Si composites was of a semiconducting type in the wide temperature range 25–1073 K.25 As it was noted in the Introduction, bamboo-wood is characterized by the presence of closed cells that impede the complete infiltration of Si and most probably prevent the formation of interconnecting Si-filled channel network. Thus, the ρ(T) dependence of MDF-SiC/Si is similar to that of the SiC/Si composites derived from the wood with open porosity. As demonstrated below, the electrical resistivity of the MDF-SiC/Si composite is more than 2 orders of magnitude lower than that of the MDF-SiC obtained after extraction of residual silicon. Hence similar to the case of biomorphic natural wood-derived-SiC/Si composites, 21 and 22 the resistivity of MDF-SiC/Si composite is determined mainly by silicon.

Typical dependences of ρ(T) for MDF-SiC are shown in Fig. 4a. To compare ρ(T) dependences of MDF-SiC and of bio-SiC derived from natural wood, it is necessary to correct for their porosity. We assume that similar to the case of natural wood precursors, 21 and 22 the porosity of the final MDF-SiC is about the same as that of the MDF-C precursor. We estimated ρ1(T) dependence of MDF-SiC in the same way as it was done for the MDF-C samples. The obtained ρ1(T) dependence for the MDF-SiC is shown in Fig. 4b (curve 3). The ρ1(T) dependence of MDF-SiC is similar to that for the wood-derived bio-SiC (eucalyptus21 and beech22) (Fig. 4b). At room temperature, the electrical resistivity ρ300 of different MDF-SiC samples fabricated from

MDF (0.8 g/cm3 density) was found to be in the range 0.12–0.2 Ω cm that is consistent with the ρ300 values for the wood-derived bio-SiC (Table 1).

The carrier concentration N can be derived from Hall coefficient (R) measurements in a magnetic field. Fig. 5 plots the dependence of the Hall voltage UR on magnetic field H measured at 77 K for MDF-SiC. Generally the value of the Hall coefficient R is derived from the low-field parts where R ∼ UR/H ≈ const.22 Then the concentration of carriers can be found as N = 1/eR (e is the electron charge) and their mobility as μ = R/ρ. The estimation of carrier concentration from the linear part of the UR(H) dependence yields N ≈ 1.6 1020 cm−3 that is approaching to 'metallic' concentration. The obtained N-value in MDF-SiC is higher by about one order of magnitude than the carrier concentration in the beech wood-derived SiC (Table 1). The thermopower measurements showed electron conduction (n-type) in MDF-SiC. Estimation of integrated mobility μ = R/ρ at 4.2 K yields very low value μ ≈ 0.4 cm2 V−1 s−1 which is comparable with the mobility in beech wood-derived SiC (Table 1).

High carrier concentration (approaching metallic concentration) in combination with electrical resistivity growth with decreasing temperature cannot be explained by classical scattering mechanism. Similar electrical transport characteristics were found also for the pine wood-derived biocarbon31 and the beech wood-derived bio-SiC22 and were explained by quantum effects which arise when charge transport occurs in disordered systems. The structural inhomogeneities can restrict dramatically the free path of electrons leading thereby to the necessity to take into account the quantum corrections to the conductivity, such as interference of electron with itself (the correction of weak localization) or mutual electron interference (the correction of electron-electron interaction).26 Structural inhomogeneities were identified as nano-crystallites in nano-amorphous biocarbon30 and 31 and as 'colonies' of nano-sized SiC grains in the beech wood-derived SiC.22 The conductivities of nano-amorphous biocarbon31 and the beech wood-derived SiC22 were well described with regard to the quantum corrections to conductivity. Since the final fine microstructure of biomorphic SiC depends on pore size of wood-derived cabon precursors,14 we performed electron microscopy studies of microstructure specificities for MDF-SiC.

Fig. 6 presents an electron microscopy image of the typical microstructure of the MDF-SiC samples, which demonstrates the presence of micro- and nanocrystallineSiC and residual amorphous carbon. Estimation of the grain size L yields L ≈ 10–70 nm for nano-SiC and L ≈ 1–10 μm for the micro-SiC. The miscrostructure of MDF-SiC is very similar to that of the natural wood-derived SiC. 12, 14 and 22

Thus, electrical charge transport through the nanocrystalline regions can result in the contribution of quantum effects to resistivity that requires taking into account quantum corrections to conductivity26 and explains non-classical (non-metallic) ρ(T) dependences for MDF-SiC with nearly 'metallic' carrier concentration. The resistance of MDF-SiC can be also mediated by charge transport through residual amorphous carbon layers which were shown 32 and 33 to contain graphite-like nanocrystallites.

3.2. Elevated-temperature studies

The studies of electrical properties at elevated temperatures from 300 to 1300 K were carried out on the samples obtained on the base of the initial MDF boards with different densities from 0.6 to 0.8 g/cm3. The content of Si the MDF-SiC/Si samples varies in the limits 30–50 vol. %.

We measured the temperature dependences of resistivity for the MDF-SiC/Si composites and appropriate porous MDF-SiC samples in the temperature range 300–1300 K. Typical ρ(T) dependences of MDF-SiC/Si composites and porous MDF-SiC are shown in Fig. 7a and b, respectively. The values of room temperature resistivity vary in a wide range from 0.08 to 0.2 Ωcm for the MDF-SiC samples and from 0.003 to 0.015 Ωcm for the MDF-SiC/Si samples. Such rather high variation in the ρ300 values for different samples of the same material is caused by difference in density (porosity) of the initial MDF precursors and in the amount of unreacted residual carbon and the Si content (for the MDF-SiC/Si composites). Despite this difference all the ρ(T) dependences of MDF-SiC samples follow semiconducting patterns in the whole temperature range 300–1300 K as well as at low temperatures (5–300 K). However, the ρ(T) dependences of the composite changes metallic pattern for the semiconducting pattern beginning at T = 500–600 K as the temperature increases. Such change in the conductivity type of the MDF-SiC/Si composite with increasing T most likely occurs because the contributions of both components (MDF-SiC and Si) become comparable near 500 K and then MDF-SiC matrix can determine the character of conductivity of the composite. Thus, conductivity of MDF-SiC/Si composite is determined mainly by Si component at low temperatures, whereas MDF-SiC matrix is more responsible for the composite conductivity at high temperatures (>500 K).

4. Conclusions

The present investigation has shown that temperature dependence of resistivity for MDF-SiC/Si composite has signature of metallic character just as for biomorphic SiC/Si composites derived from natural wood with open porosity (eucalyptus, beech, sapele). The conductivity of SiC/Si in the temperature range 5–500 K originates primarily from silicon residing in cellular pores of the MDF-SiC matrix. Such pores filled by Si seem to form interconnecting network. Because of its dependence on residual porosity and the Si content, the resistivity of MDF-SiC/Si composite at room temperature varies in a range from 0.003 to 0.02 Ω cm.

Similar to natural wood-derived bio-SiC materials, the ρ(T) dependence of porous biomorphic MDF-SiC has semiconducting character, i.e. the electrical resistivity grows with decreasing temperature in the whole temperature range 5–1300 K. The main charge transfer parameters in MDF-SiC have been determined by Hall method: the carriers are n-type with concentration ∼1020 cm−3 and very low mobility ∼0.4 cm2 V−1 s−1.

In MDF-SiC, the contradiction between the high bulk carrier concentration approaching the metallic one and semiconducting type of the ρ(T) dependence is explained by quantum effects which arise in disordered conducting systems and contribute to the resistivity. Our TEM studies did reveal the presence of disordering elements in the structure of MDF-SiC, specifically nanocrystallineSiC regions, charge transfer through which can result in the necessity of accounting quantum corrections to the conductivity. The transport in MDF-SiC occurs similarly to that in the bio-SiC derived from eucalyptus21 and beech.22

At T > 500 K, the character of the ρ(T) dependence of MDF-SiC/Si composite changes from metallic to semiconducting type. This seems to occur because at high temperatures the contribution of MDF-SiC matrix to the conductivity of MDF-SiC/Si composite becomes substantial and even more decisive compared with the contribution of Si component.

Acknowledgements

This study was supported by the Russian Basic Research Foundation (project no. 7-03-91353NNF_a), the Presidium of the Russian Academy of Sciences (program no. P-03), and the Spanish Projects MAT 2007-30141-E and PET 2006-0658.

References

1.H. Sieber, C. Hoffmann, A. Kaindl, P. Greil

Biomorphic cellular ceramics

AdvEng Mater, 2 (2000), pp. 105–109

2. T. Kosolapova

Carbides properties, production and applications

Plenum Press, New York, London (1971)

3. C. Forrest, P. Kenedy, J. Shennam

The fabrications and properties of self-bonded silicon carbide

Special Ceram, 5 (1972), pp. 99–123

4. O. Chakrabati, S. Ghosh, J. Mukerji

Influence of grain size, free silicon content and temperature in the strength and thoughness of reaction bonded silicon carbide

Ceram Int, 5 (2) (1991), pp. 118–123

5. S. Prochazka

The role of boron and carbon in the sintering of silicon carbide

Special Ceram Br Ceram Res Assoc, 6 (1975), pp. 171–181

6. C. Greskovic, J.H. Rosolowski

Sintering of covalent solids

J Am Ceram Soc, 59 (7–8) (1976), pp. 336–343

7. T. Ota, M. Takahashi, T. Hibi, M. Ozawa, S. Suzuki, Y. Hikichi

Biomimetic process for producing SiC “Wood”

J Am Ceram Soc, 78 (12) (1995), pp. 3409–3411

8. P. Greil, T. Lifka, A. Kaindl

Biomorphic cellular silicon carbide ceramics from wood. I. Processing and microstructure

J Eur Ceram Soc, 18 (1998), pp. 1961–1973

9. P. Greil, T. Lifka, A. Kaindl

Biomorphic cellular silicon carbide ceramics from wood: II. Mechanical properties

J Eur Ceram Soc, 18 (1998), pp. 1975–1983

10. J. Martinez-Fernandez, F.M. Varela-Feria, M. Singh

High temperature compressive mechanical behavior of biomorphic silicon carbide ceramics

Scr Mater, 43 (813–818) (2000)

11. J. Martínez-Fernández, F.M. Varela-Feria, A. Domínguez Rodríguez, M. Singh

Microstructure and thermomechanical characterization of biomophic silicon carbide-based ceramics

Environment conscious materials; ecomaterialsCanadian Institute of Mining, Metallurgy, and Petroleum (2000) pp. 733–740, ISBN:1-894475-04-6

12.A.R. de Arellano-López, J. Martínez-Fernández, P. González, C. Domínguez, V. Fernández-Quero, M. Singh et al.

SiC: a new engineering ceramic material

Int J Appl Ceram Technol, 1 (1) (2004), pp. 56–67

13.F.M. Varela-Feria, J. Martinez-Fernandez, A.R. de Arellano-Lopez, M. Singh

Low density biomorphic silicon carbide: microstructure and mechanical properties

J Eur Ceram Soc, 22 (2002), pp. 2719–2725

14. F.M. Varela-Feria, J. Ramırez-Rico, A.R. de Arellano-Lopez, J. Martınez-Fernandez, M. Singh

Reaction–formation mechanisms and microstructure evolution of biomorphic SiC

J Mater Sci, 43 (2008), pp. 933–941

14. H. Robbins, B. Schwartz

Chemical etching of silicon

J ElectrochemSoc, 106 (6) (1959), pp. 505–508

16. V.S. Kaul, K.T. Faber, R. Sepulveda, A.R. de Arellano-Lopez, J. Martinez-Fernandez

Precursor selection and its role in the mechanical properties of porous SiC derived from wood

Mater SciEng A, 428 (2006), pp. 225–232

17. M. Presas, J.Y. Pastor, J. Llorca, A.R. de Arellano-Lopez, J. Martınez-Fernandez, R.E. Sepulveda

Mechanical behavior of biomorphic Si/SiC porous composites

Scr Mater, 53 (2005), pp. 1175–1180

18.T.S. Orlova, B.I. Smirnov, A.R. de Arellano-Lopez, J. Martínez-Fernández, R. Sepulveda

Anisotropy of electric resistivity of sapele-based biomorphic SiC/Si composites

FizTverdTela (St. Petersburg), 47 (2) (2005), pp. 220–223 [Phys Solid State 2005;47(2):229–32]

19. L.S. Parfen'eva, T.S. Orlova, N.F. Kartenko, N.V. Sharenkova, B.I. Smirnov, I.A. Smirnov et al.

Thermal conductivity of the SiC/Si biomorphic composite, a new cellular ccoceramic

FizTverdTela (St. Petersburg), 47 (7) (2005), pp. 1175–1179 [Phys Solid State 2005;47(7):1216–20]

20. L.S. Parfen'eva, T.C. Orlova, B.I. Smirnov, I.A. Smirnov, H. Misiorek, J. Mucha et al.

Anisotropy of the thermal conductivity and electrical resistivity of the SiC/Si biomorphic composite based on a white-eucalyptus biocarbon template

FizTverdTela (St. Petersburg), 48 (12) (2006), pp. 2157–2164 [Phys Solid State 2006;48(12):2281–88]

21. T.S. Orlova, D.V. Il'in, B.I. Smirnov, I.A. Smirnov, R. Sepulveda, J. Martinez-Fernandez et al.

Electrical properties of bio-SiC and Si components of the SiC/Si biomorphic composite

FizTverdTela (St. Petersburg), 49 (2) (2007), pp. 198–203 [Phys Solid State 2007;49(2):205–10]

22. V.V. Popov, T.S. Orlova, J. Ramirez-Rico, A.R. de Arellano-Lopez, J. Martinez-Fernandez

Electrical properties of the SiC/Si composite and the biomorphic SiC ceramic fabricated from Spanish beech wood

FizTverdTela (St. Petersburg), 50 (10) (2008), pp. 1748–1753 [Phys Solid State 2008;50(10):1819–25]

23. A.I. Shelykh, B.I. Smirnov, T.S. Orlova, I.A. Smirnov, A.R. de Arellano-Lopez, J. Martinez-Fernandez et al.

Electrical and thermoelectric properties of the SiC/Si biomorphic composite at high temperatures

FizTverdTela (St. Petersburg), 48 (2) (2006), pp. 214–217 [Phys Solid State 2006;48(2):229–32]

24.F.M. Varela-Feria, J. Martínez-Fernández, A.R. de Arellano López, M. Singh

Precursor selection for properties optimization in biomorphic SiC ceramics

Ceram SciEngProc, 23 (4) (2002), pp. 681–685

25. D. Mallick, Om.Chakrabarti, D. Bhattacharya, M. Mukherjee, H. Maiti, R. Majumdar

Electrical conductivity of cellular Si/SiC ceramic composites prepared from plant precursors

J ApplPhys, 101 (2007) 0033707-1–0033707-7

26. V.F. Gantmakher

Electrons and disorder in solids (Fizmatlit Moscow, 2003)

Oxford University Press, Oxford, MS, United States (2005)

27.M.A. Bautista, A.R. de Arellano-Lopez, J. Martnez-Fernandez, A. Bravo-Leon, J.M. Lopez-Cepero

Optimization of the fabrication process for medium density fiberboard (MDF) – based biomimetic SiC

Int J Refractiry Met Hard Mater, 27 (2009), pp. 431–437

28. Bautista MA. Master Degree Thesis. Sevilla, Spain: Universidad de Sevilla; 2006.

29. A.K. Kercher, D.C. Nagle

Evaluation of carbonized medium-density fiberboard for electrical applications

Carbon, 40 (2002), pp. 1321–1330

30. L.S. Parfen'eva, T.S. Orlova, N.F. Kartenko, N.V. Sharenkova, B.I. Smirnov, I.A. Smirnov et al.

Thermal and electrical properties of a white-eucalyptus carbon preform for SiC/Si ecoceramics

FizTverdTela (St. Petersburg), 48 (3) (2006), pp. 415–420 [Phys Solid State 2006;48(3):441–46]

31. V.V. Popov, T.S. Orlova, J. Ramirez-Rico

Electrical and galvanomagnetic properties of biocarbon preforms of white pine wood

FizTverdTela (St. Petersburg), 51 (11) (2009), pp. 2118–2122 [Phys Solid State 2009;51(11):2247–51]

32. C.E. Byrne, D.C. Nagle

Carbonized wood monoliths – characterization

Carbon, 35 (2) (1997), pp. 267–273

33. A.K. Kercher, D.C. Nagle

Microstructural evaluation during charcoal carbonization by X-ray diffraction analysis

Carbon, 41 (2003), pp. 15–27

Figure captions

Figure 1.SEM micrographs of MDF-C taken perpendicular (a) and parallel (b) to the direction of compacting the parent MDF boards.

Figure 2.Temperature dependences of resistivity of porous biocarbon derived from MDF board (1), white pine (curve 2 from Ref.31) and eucalyptus (curve 3 from Ref.30) woods without (a) and with (b) correction for the porosity.

Figure 3.(a) Temperature dependence of the electrical resistivity of MDF-SiC/Si composite (with 30 vol.% of Si). (b) Comparison of temperature dependences of the electrical resistivity of MDF-SiC/Si composite (curve 1) with 30 vol.% of Si and of the bio-SiC derived from eucalyptus (curve 2 from Ref.21) and from beech (curve 3 from Ref.22).

Figure 4. (a) Temperature dependences of the electrical resistivity of MDF-SiC samples which were obtained on the base of the same MDF board, but their MDF-precursors were cut from its different parts. (b) Temperature dependences of the electrical resistivity of bio-SiC samples derived from eucalyptus (1), beech (2) and MDF board (3), which are plotted with correction for the samples porosity.

Figure 5.Dependence of the Hall voltage UR at 77 K on the magnetic field H for MDF-SiC. Dashed line corresponds the linear dependence UR(H).

Figure 6.Electron microscope image of the MDF-SiC demonstrating the presence of micro- and nanocrystallineSiC and residual amorphous carbon.

Figure 7. (a) Temperature dependences of the electrical resistivity for MDF-SiC/Si composite derived from MDF boards with the density in the 0.6–0.8 g/cm3 limits and Si content in the 20–50 vol.% range. (b) Temperature dependences of the electrical resistivity of two MDF-SiC samples which were obtained on the base of the same MDF board (the density 0.8 g/cm3), but their MDF-precursors were cut from its different regions.

Table 1

Table 1. Comparison of average values of porosity P, resistivity at room temperature ρ_{300} with and without correction for the porosity, ratio $\rho_{5\,K}/\rho_{300\,K}$ of resistivity values at 5 and 300 K, type and concentration N of charge carriers in the bulk for porous biomorphic SiC, processed on the base of different precurcors.

Sample	**Porosity**	$\rho_{300\,K}$ **(Ω cm) without correction for the porosity**	$\rho_{300\,K}$ **(Ω cm) with correction for the porosity**	$\rho_{5\,K}/\rho_{300\,K}$	**Type of chargecarriers**	**Concentration** N **of carriers** (cm^{-3})	**Mobility** μ **of charge carriers** ($cm^2\ V^{-1}\ s^{-1}$)	**Source**
Eucalyptuswood-derivedSiC	43%	1.3	0.75	2	–	–	–	[21]
Beechwood-derivedSiC	47%	0.4	0.2	1.8	*n*-type	$\sim 10^{19}$	0.8	[22]
MDF-SiC	50%	0.3	0.12–0.15	1.7	*n*-type	1.6×10^{20}	0.4	Thepresentpaper

Figure 1

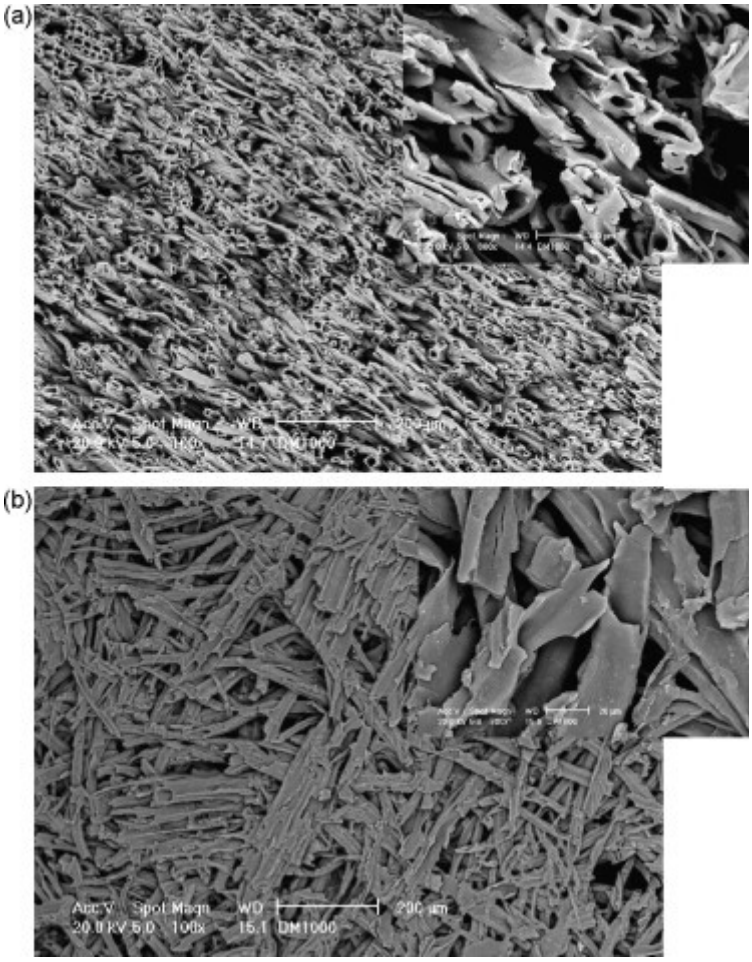

Figure 2

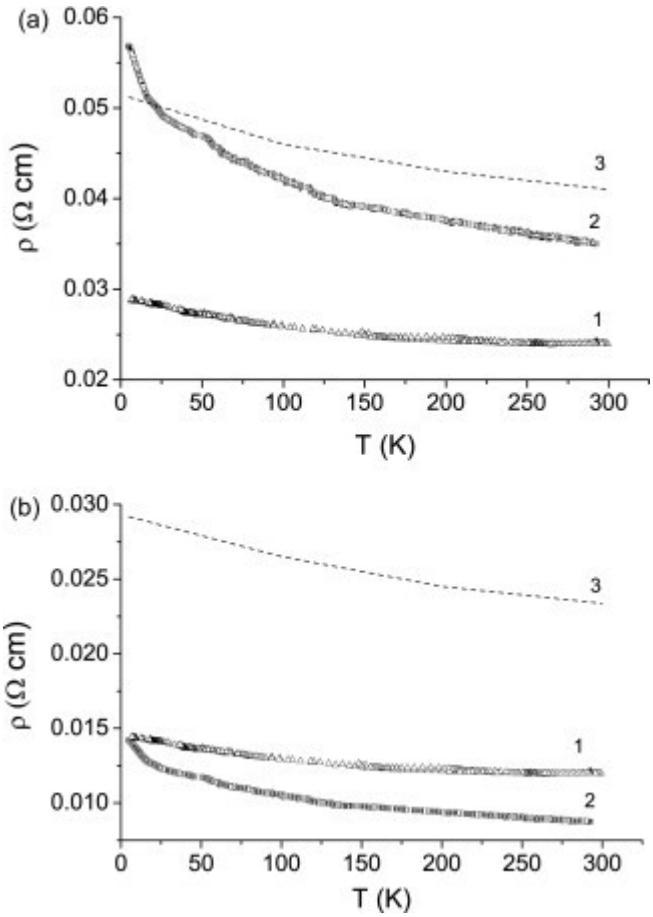
(a)
0.06
0.05
0.04
0.03
0.02
ρ (Ω cm)
3
2
1
0
50
100
150
200
250
300
T (K)
(b)
0.030
0.025
0.020
0.015
0.010
ρ (Ω cm)
3
1
2
0
50
100
150
200
250
300
T (K)

Figure 3

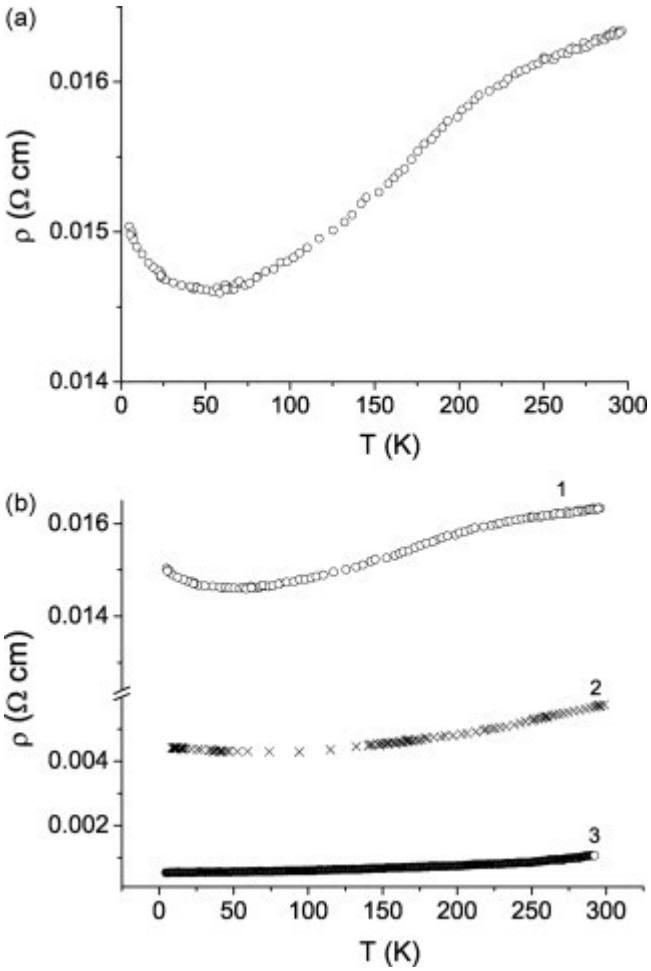
(a)
0.016
0.015
0.014
ρ (Ω cm)
0
50
100
150
200
250
300
T (K)
(b)
1
2
3
0.016
0.014
0.004
0.002
ρ (Ω cm)
0
50
100
150
200
250
300
T (K)

Figure 4

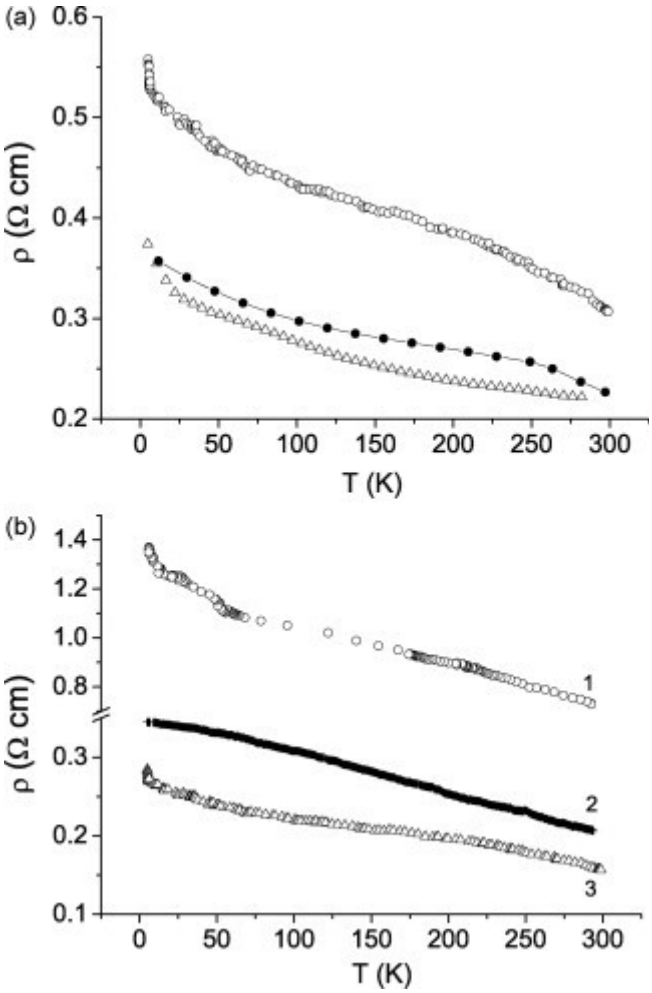

Figure 5

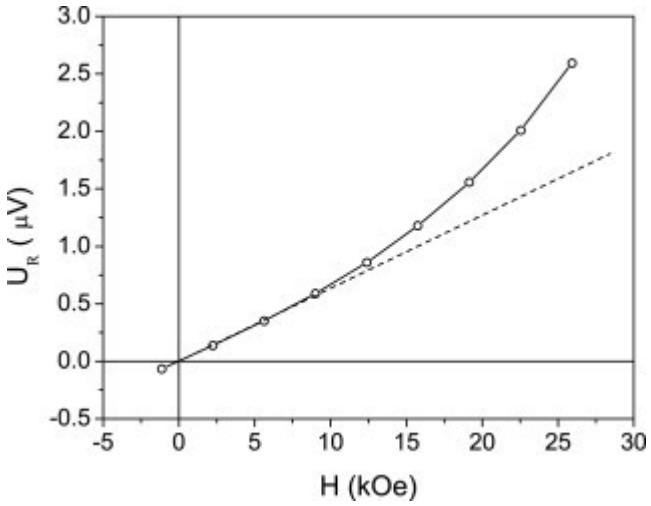

Figure 6

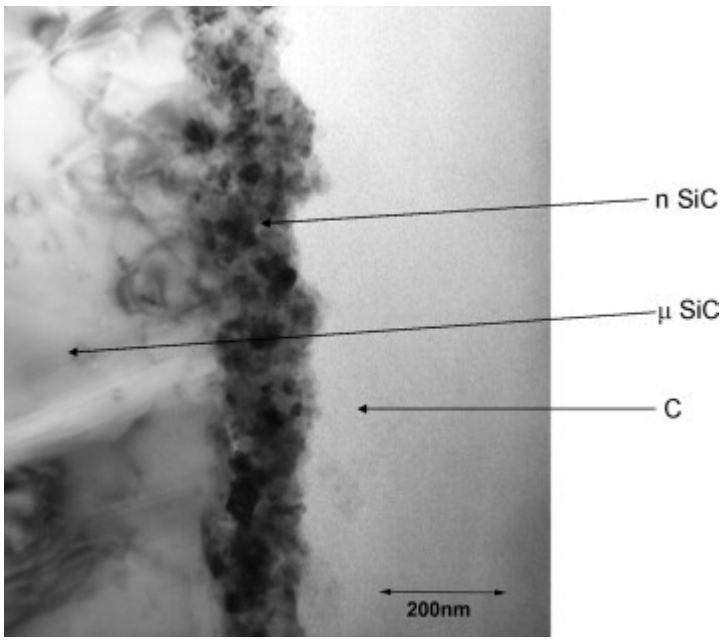

Figure 7

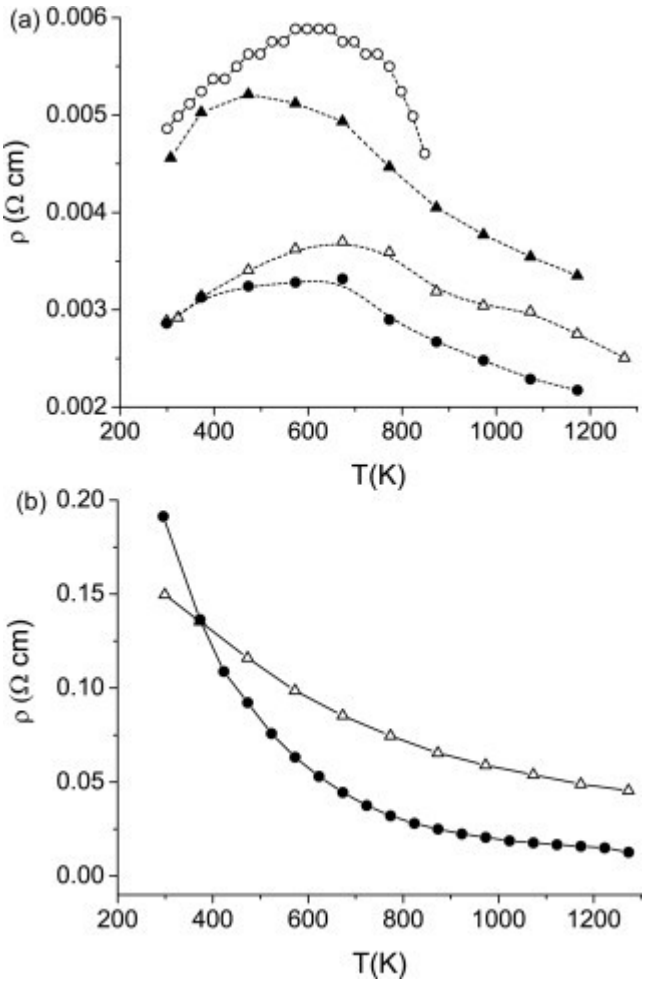
(a)
0.006
0.005
0.004
0.003
0.002
ρ (Ω cm)
200
400
600
800
1000
1200
T(K)
(b)
0.20
0.15
0.10
0.05
0.00
ρ (Ω cm)
200
400
600
800
1000
1200
T(K)